

Numerical Analysis Of Aerofoil Shape Propeller Boss Cap Fin (PBCF) To Improve Propeller Efficiency

Pritam Majumder, Subhendu Maity

Abstract: Scarcity in fossil fuel and other environmental issues forced researchers to search ways to improve in the efficiency of the marine vehicle which is considered the most efficient and economic transport medium now a day. Energy saving device (ESD) is such an implementation to keep dominant impact in this aspect. This paper investigates the effect of aerofoil shape propeller boss cap fin (PBCF) as ESD computationally. Based on Reynolds-averaged Navier-Stokes (RANS) equations, numerical simulations have been performed to increase propeller efficiency with aerofoil shape propeller boss cap fin in computational fluid dynamic (CFD) approach. In this study, four separate aerofoil shape PBCF with different NACA profile (NACA4412, NACA0012, NACA1412, NACA2412) has been used to find a suitable profile for PBCF. Numerical results shows aerofoil shape PBCF with NACA4412 effectively improves propeller performance by improving the efficiency by approximately 3.52% than parent propeller. The pressure distribution elaborate PBCF (NACA4412) creates a high pressure difference between the pressure side and suction of the propeller as well as high thrust generation. Besides that velocity field, swirl strength are also studied to get and understand the details of involved flow phenomenon.

Keywords : Thrust coefficient, torque coefficient, PBCF, propeller efficiency, hub vortex, swirl strength.

I. INTRODUCTION

With growing population and globalization, water medium transport system has become a more effective transport mode due to its economic benefit and lesser environmental issues compared to other medium^[1]. Marine vehicles faced various off design environmental conditions while moving in sea and losses in energy as well as efficiency. Energy saving devices (ESD) has been used widely now days to improve ship power performance by decreasing energy loss during its manoeuvring. These devices help to overcome issues like cavitation, vibration, noise formation etc.^[2]. ESDs are generally installed before, after or in between these two positions of a propeller to improve inflow as well as out flows from it. Propeller is the most predominant part in ship propulsion to generate propulsive power. Performance predication for a marine propeller therefore becomes a vital aspect for ship design in various off design as well as normal condition. A propeller usually performs in a non-uniform flow field due to generation of wake by hull and other parts of the

ship^[3]. A marine propeller generally produces a high propulsive efficiency, but induced swirling motion from rotating propeller drastically reduces the energy for ship propulsion system. Recovering the energy losses due to rotational motion become a challengeable task and has studied by various authors. Counter rotating propeller, fixed guide vane propeller, duct propellers are some of the concept to overcome these issues which are also perfect from hydrodynamic point of view^[4]. Propeller boss cap fins (PBCF) are one of the most efficient ESD to improve propeller efficiency as well as consume less fuel through the reduction of hub vortex and rudder induced cavitation. In PBCF small fins are attached with boss cap of the propeller to recover energy loss due to hub vortex. It improves propeller efficiency by reducing the required torque and increasing produced thrust^[5]. According to MOL Techno Trade Ltd. Report (19th May 2017) PBCF can improve propeller efficiency up to 5%. There are equal amount of reduction in CO₂ emission at the same rate as fuel consumption reduction and effective noise reduction as per their report^[6].

In this paper, model scale numerical investigation has been performed to observe the effect of PBCF to increase propeller efficiency. Based on Reynolds Average Navier Stoke (RANS) equation numerical simulations have been carried out for modified aerofoil shape PBCF in open water test condition in ANSYS Fluent 18.0 software. The obtained results are compared with experimental work to ensure the validation of the numerical solver. Based on obtained results best profile PBCF is selected for numerical simulation and to investigate fluctuation of pressure, velocity, swirl strength, vortexes

II. BACKGROUND

2.1 Propulsive characteristic

For the prediction of propeller performance, consideration of its practical hydrodynamic environment is very essential. A propeller analysis is generally performed in open water i.e. in uniform flow with steady load condition or after hull environment where it works in steady and unsteady load condition with mixed wake field region generated due to hull resistance and other accessories^[1].

According to blade element theory, when a propeller blade element moves through water,

it is subjected to an axial velocity component (V_A) as well as tangential velocity component (πnD), [n and D respectively revolution per second and propeller diameter] which results in an implementation of

Revised Manuscript Received on January 05, 2020

* Correspondence Author

Pritam Majumder*, Dept. of Mechanical Engg., Research scholar, NIT Meghalaya, Shillong, India,

Subhendu Maity, Dept. of Mechanical Engg., Assistant Professor, NIT Meghalaya, Shillong,

a resultant velocity on the blade element. This resultant velocity generates a force on the blade element. The axial component of that force is known as thrust (T) and the tangential component which generates a moment around the propeller axis is known as torque (Q). These two parameters are basically the main parameters to analyse propeller performance in open water condition considering effect of water wave is negligible and propeller is deeply submerged in water. These parameters are usually expressed in non-dimensional term known as thrust coefficient (K_T) and torque coefficient (K_Q). Advance velocity is represented by non-dimensional term known as advance coefficient (J). The above mentioned coefficients are analytically expressed as below-

$$K_T = \frac{T}{\rho n^2 D^4} \dots\dots\dots(1)$$

$$K_Q = \frac{Q}{\rho n^2 D^5} \dots\dots\dots(2)$$

$$J = \frac{V_A}{nD} \dots\dots\dots(3)$$

Where ρ is water density.
Propulsion efficiency (η) of the propeller depends on thrust and torque coefficient and is expressed as

$$\eta = \frac{K_T}{K_Q} \times \frac{J}{2\pi} \dots\dots\dots(4)$$

Graphical representation of thrust and torque coefficient over a wide range of advance coefficient helps to identify the optimum efficiency in propeller curve

III. LITERATURE REVIEW

In this section a brief background study have been conducted about the ESDs to analyse their impact on propeller performance improvement. Authors tried to establish their concept through experimental approach, numerical investigations as well as analytical observations. Walker^[7] in his PhD work performed experimental investigations to observe influence of cavitations and blockage for ice class propeller (surrounded by ice). Experiments were performed in a cavitation tunnel, for open propeller and ducted propeller over a wide range of cavitation number, and also in a towing tank for uniform flow and ice blocked condition. It is observed that blockage enhances mean load in both propellers thrust (K_T) and torque (K_Q) coefficients for open propeller are increased by 300% and 106% respectively at advance coefficient (J) 0.7. In case of ducted propeller the coefficients are enhanced to 230% and 175% respectively at J= 0.3. It is also observed that cavitation reduces mean load with increase in mean flow oscillation (mean K_T and K_Q are reduced by 37% and 31% respectively at J= 0.2, when the cavitation number is decreased from 13.5 to 1.8). Nojiri *et al.*^[8] experimentally as well as numerically explained the detailed physics of working of a PBCF. They experimentally investigated effect of 4, 5, 6 bladed PBCF and found around 1.5% efficiency improvement than conventional propeller. According to their study velocity drastically reduces at fin root zone which helps to destroy the generated hub vortex toward propeller centre axis. Pressure distribution from numerical simulation also explained the

thrust improvement, torque reduction as well as efficiency improvement from numerical simulation. Besides that numerical simulations also suggested optimizing PBCF size for further improvement in performance by reducing frictional losses in the aft and outer part of the fin. Kawamura *et al.*^[9] investigated the effect of Reynolds number and hull developed wake on PBCF through computational approach in model scale as well as full scale. Computational results show combined effect of Reynolds number and hull wake significantly affects propeller efficiency with PBCF in full scale. This happens because of reduction of fin as well as boss drag with combined effect in PBCF and they claimed maximum 2.32% efficiency improvement. Hydrodynamic performance of PBCF of a controllable pitch propeller has been analysed by Xiong *et al.*^[10] by RANS method. Besides that, the effect of aerofoil shape PBCF and axial as well as angular position installation were also observed to identify the shape of the PBCF and optimum position respectively. Aerofoil shape PBCF helped dominantly to improve propeller efficiency. To find the correlation between the various design parameter of PBCF at full factorial design method parametric study has been performed by Lim *et al.*^[11]. Among the six selected design parameters, installation angle and fin position contributed significant affect improving towards propeller efficiency. Alongside numerical as well as experimental investigations had been observed to study the effect of divergence cap in performance of propeller with PBCF. Divergence cap with PBCF provide insignificant effect by decreasing propeller efficiency in maximum cases. Cavitation study shows at the aft part of propeller hub vortex raises with divergence cap and results in increased torque requirement without any significant change in thrust. The effect of HI-Fin in propeller efficiency has been investigated by Park *et al.*^[12] using CFD approach. Parametric study shows that fin area, pitch angle and phase angle are the most effective design parameters to optimize fin size. Negative pressure significantly reduces with HI- Fin to reduce hub vortex. Stereoscopic particle image velocimetry (SPIV) and CFD result show similar result in case of tangential velocity, axial velocity and vorticity contour. Results show HI- Fin helps to increase axial velocity and reduce tangential velocity as well as vorticity. Self-propulsion test shows HI-Fin reduces the thrust by a small amount but comparatively reduces high torque. There is increase in efficiency and overall reduction of power consumption by 1.8%- 2%. Numerical as well as experimental investigation performed by Sun *et al.*^[13] to observe the impact of PBCF to improve propeller efficiency in propeller rudder system. Results of cavitation test represented 1.47% energy saving with PBCF in absence of rudder at an advance ratio 0.8. Numerical simulations indicate with the introduction of ordinary rudder and twisted rudder with PBCF decreases propeller energy saving considerably up to 1.08% and 1.16% respectively due to interface effect of PBCF as well as generation of a negative thrust. To increase propulsive efficiency, PBCF were introduced by Mizzi *et al.*^[14] that were optimized for full scale propeller along with CFD simulation. For the study, 120 different PBCF design at full scale were analyzed by coupling numerical model with optimization parametric modeler with open source model scale Potsdam propeller VP1304. Results show there is 3% accuracy in open water test for advance coefficient of 0.6 to 1 and beyond that due to avoidance of

transition zone there is much error. At advance ratio 0.8 (optimum condition), thrust, torque and efficiency were observed and compare with no fin condition. There is 2.5% gain in thrust coefficient, 1.4% increase in torque coefficient and 1% increase in efficiency. When the blade pitch as well as fin pitch is equal, optimum results were obtained. After 120 PBCF analyses, it was found that 1.3 % increase in energy efficiency was gained gain at optimum design condition. With the use of PBCF, hub vortex reduces greatly by obstructing velocity at the root area.

IV. PROPELLER GEOMETRY

3.1 Validation study of the model

For numerical study, an open source controllable pitch propeller VP1304 [fig. 1] [15], developed by SVA Potsdam Model Basin in Germany in 1998 is used. Numerically obtained results were compared with experimental work performed in Potsdam Propeller Test Case (PPTC) reported by SVA. The various geometric parameters of the model scale propeller have been mentioned in table 1.

Table 1 Various geometric parameter details of VP1304 propeller [15]

Type	Symbol	Unit	Value
Diameter	D	m	0.250
Pitch ratio (r/R=0.7)	P _{0.7} /D	----	1.635
Area ratio	A _E /A _O	----	0.779
Chord length	C _{0.7}	m	0.104
Skew	θ	°(deg)	18.837
Hub ratio	D _h /D	----	0.300
No.of blade	Z	----	5
Rotation	Direction	----	Right
Revolution per second	n	/sec	15

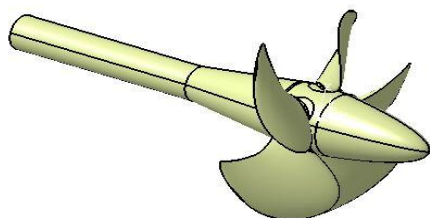


Fig. 1 VP1304 Propeller [8]

3.2 Mesh generation

In this computational analysis, mesh has been generated in ANSYS 18.0 mesh module. To achieve more accurate results, proper mesh generation is a key factor. Although structural mesh provide more accurate results compared to unstructured mesh, due to complex geometry a cut cell assembly type mesh are utilised for mesh generation. This type of mesh is preferable compared to the conventional mesh due to its less computational time requirement and better quality mesh in case of complex geometry. Local refinements are also performed at the sharp edge and complex surfaces of the propeller through appropriate edge, surface and body sizing to achieve accurate results.

Since the flow domain near the solid boundary of the propeller is mostly affected by a viscous zone, a very fine mesh is generated in that zone and the mesh gradually increases in size towards far field zone. Although for capturing near wall surface effect i.e laminar sub layer study

and to avoid the buffer zone, y⁺ value should be kept below 1, but due to limited computer resources y⁺ value is kept at little high value. The detailed view of the generated mesh has been shown in fig. 2.

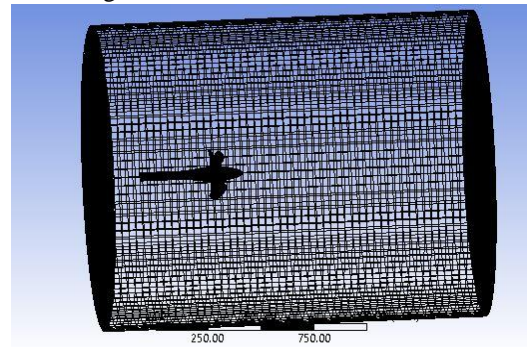


Fig. 2 mesh generation

V. COMPUTATIONAL DETAILS

4.1 Governing equation

Finite volume based CFD commercial tool (ANSYS FLUENT 18.0) has been used for numerical simulation. This tool considered a prominent commercial package since long and is widely used for research work on propeller performance analysis. Considering the effect of time calculation numerical simulations are performed on Reynolds Average Navier Stokes (RANS) equations, which significantly consider the rapid fluctuation of pressure surrounding the propeller with respect to time.

Conservation of mass in every principal axis is represented as:

$$\frac{\partial}{\partial x_i}(\rho \bar{u}_i) = 0 \dots \dots \dots (5)$$

Here fluid density is expressed as ρ, average velocity in each principal direction is \bar{u}_i , and x_i is the cartesian coordinate.

In each principal direction momentum conservation is written as equation (6)

$$\frac{\partial}{\partial t}(\rho \bar{u}_i) + \frac{\partial}{\partial x_j}(\rho \bar{u}_i \bar{u}_j + \overline{\rho u'_i u'_j}) = -\frac{\partial \bar{p}}{\partial x_i} + \frac{\partial \tau_{ij}}{\partial x_j} + G_i + F_i \dots \dots \dots (6)$$

Body force and gravitational force are expressed as F_i and G_i respectively. \bar{p} is mean pressure. Both the forces have been neglected in this study whereas mean viscous stress tensor, represented as $\bar{\tau}_{ij}$ is defined as

$$\bar{\tau}_{ij} = \mu \left(\frac{\partial \bar{u}_i}{\partial x_j} + \frac{\partial \bar{u}_j}{\partial x_i} \right) - \frac{2}{3} \mu \frac{\partial \bar{u}_k}{\partial x_k} \delta_{ij} \dots \dots \dots (7)$$

In this equation δ_{ij} is known as Kronecker delta. It becomes unity when the value of i and j are unique and zero in case of others. Based on equation (5) and (7), RANS equation finally become as follow

$$\frac{\partial}{\partial t}(\rho \bar{u}_i) + \frac{\partial}{\partial x_j}(\rho \bar{u}_i \bar{u}_j + \overline{\rho u'_i u'_j}) = \frac{\partial}{\partial x_j} \left[\mu \left(\frac{\partial \bar{u}_i}{\partial x_j} + \frac{\partial \bar{u}_j}{\partial x_i} \right) - \frac{2}{3} \mu \frac{\partial \bar{u}_k}{\partial x_k} \right] - \frac{\partial \bar{p}}{\partial x_i} \dots \dots \dots (8)$$

where μ and p represent respectively dynamic viscosity and pressure. The term $\overline{\rho u'_i u'_j}$ is known as Reynolds stress tensor, which comes from the average of fluctuating component of



momentum equation in turbulence flow.

There are various turbulence models to capture fluctuating component of velocity and pressure in turbulence zone. In this study Reynolds stresses are solved with SST (Shear Stress Transport) $k-\omega$ turbulence model. $k-\omega$ turbulence model plays dominant role in viscous affected zone and $k-\epsilon$ in the far field zone from the solid boundary where inertia forces are more effective. SST $k-\omega$ turbulence model consists of the combined effect of $k-\omega$ as well as $k-\epsilon$ turbulence model and hence is capable to take care of both flows about the near wall effect and far field region respectively. Here, turbulence kinetic energy (k) and specific rate of dissipation (ω) are derived by solving transport equation for k and ω respectively, whereas, ϵ is the rate of dissipation of turbulence energy, is obtained by solving transport equation for ϵ .

According to ITTC (International Towing Tank Conference) 2014, recommendation to imprisonment all the challenging features for unsteady flow condition for an incompressible flow field in numerical simulation time step size has been considered as 0.075 sec.

There are basically two approaches for numerical simulations on a propeller to identify its prominent characteristics such as thrust, torque and efficiency. One is sliding mesh method where there is a rotating fluid domain surrounding the propeller and a stationary fluid domain outside rotating fluid. Another one is known as moving reference frame (MRF) method where fluid domain surrounding the propeller remain stationary while the reference frame rotate with respect to the global reference frame. According to Mizzi *et al.* [14] work, both the approach are suitable for numerical simulation and produce approximately same result, but in this investigation, less computational time and power requirement, all the simulations have been performed with MRF approaches.

4.2 Validation study

For confirmation about the accuracy of the used numerical solver, open water propeller parameters for VP1304 controllable pitch propeller developed by SVA [15] are compared with interpolated experimental results of Owen *et al.* [1] (table 2). In this study both sliding mesh and MRF approaches are performed for validation purpose, but due to less computational time requirement and an urge to obtain more accurate results, others investigations have been performed in only MRF approach. All the obtained results for validation are shown in table 3 and 4 and also graphically represented in fig. 4 and 5.

Table 2 SVA [15] experimental results interpolated for various J value by Owen *et al.* [1]

J	K_T	K_Q	η
1	0.4010	0.09793	0.6501
0.8	0.5109	0.11821	0.5498
0.6	0.6290	0.13958	0.4295

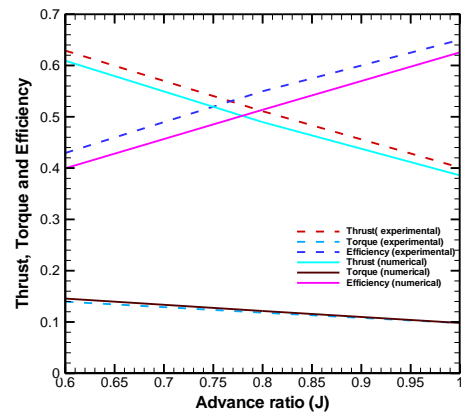


Fig.4 Validation study in sliding mesh approach

There are good agreements between experimental results and numerical (with a maximum deviation of about 7% in one case) obtained results in case of thrust, torque and efficiency at various advance ratio and thus confirm about the correctness of the numerical solver for both the MRF as well as sliding mesh approaches.

Table 3 Sliding mesh method

Adv. Ratio	K_T	Error (%)	K_Q	Error (%)	η	Error (%)
1	0.385 7	3.80	0.09815	0.22	0.625	3.57
0.8	0.489 6	4.17	0.1214	2.70	0.513	6.56
0.6	0.609 2	3.14	0.14565	4.34	0.399	6.96

Table 4 MRF method

Adv. Ratio	K_T	Error (%)	K_Q	Error (%)	η	Error (%)
1	0.424 5	5.56	0.1012	3.33	0.6679	2.73
0.8	0.485 3	5.01	0.1178	0.34	0.5247	4.56
0.6	0.633 9	0.77	0.1451	4.01	0.4171	2.88

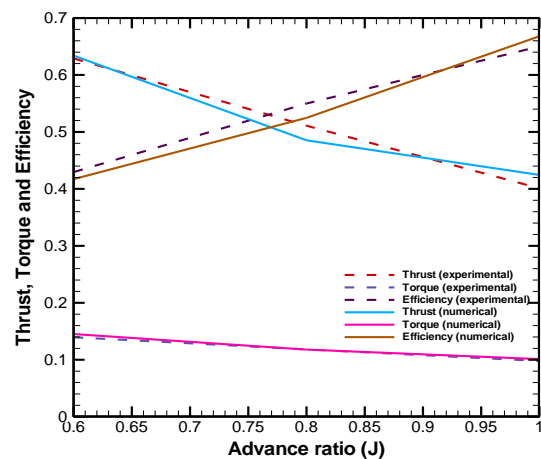


Fig. 5 Validation study in MRF approach

4.3 Grid dependency test

To investigate the influence of number of grid in numerical simulation, grid dependency test is performed for three different types of grid (coarse, medium and fine) for a particular advance ratio ($J=1$) with MRF approach for three significant parameters (K_T , K_Q and η) as

mentioned in table 5. It has been noticed that with increasing number of elements, accuracy of the obtained results is increasing gradually and it becomes approximately same after a particular number of elements as shown in fig. 6. Hence all simulation runs near about 5.5 million fine meshes.

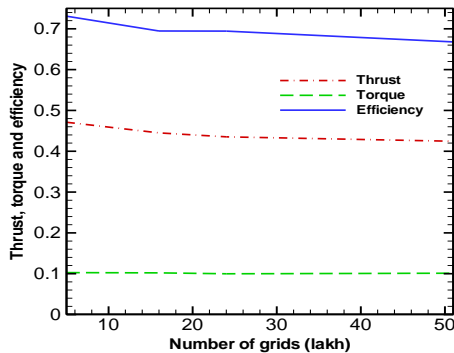


Fig.6 Grid dependency test

Table 5 Grid dependency test at J=1in MRF approach

Mesh type		K_T	Error (%)	K_Q	Error (%)	η	Error (%)
Coarse	5	0.47	17.4	0.102	4.84	0.73	12.4
Medium	16	0.44	10.9	0.102	4.22	0.69	6.86
Fine	24	0.43	8.55	0.099	1.19	0.69	6.81
Finest	51	0.42	5.56	0.101	3.33	0.66	2.73

4.4. Modified model

After the validation of model geometry, some aerofoil shape propeller boss cap fins has been introduced in model propeller. There is 1.3% efficiency improvement in propeller efficiency with rectangular fins as numerically investigated by Mizzi et al. [14]. In this paper modification has been performed in PBCF shape to obtain more efficiency improvement compared to previous study. NACA 4412 is a suitable guide vane due its less corrosion and minimum pressure difference between pressure side and suction side in case of a Francis turbine [16]. Therefore four different aerofoil shape (NACA0012, NACA1412, NACA2412, NACA4412) fins have been introduced as PBCF in ANSYS 18.0 modelling software as shown in fig 7 and fig. 8. Numbers of PBCF are equal to numbers of propeller blade and the PBCF is kept in between two adjacent blade root section. While designing the PBCF, the maximum diameter of the PBCF should not exceed 33% of the propeller diameter and it is one of the most necessary criteria in PBCF design [17]. Here the ratio of PBCF radius and propeller radius are kept 0.28.

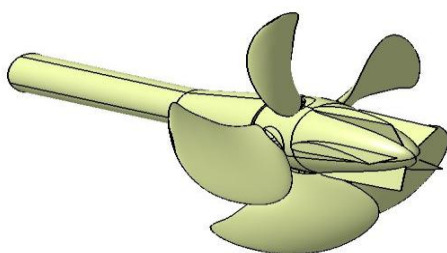


Fig. 7 Propeller with aerofoil fin

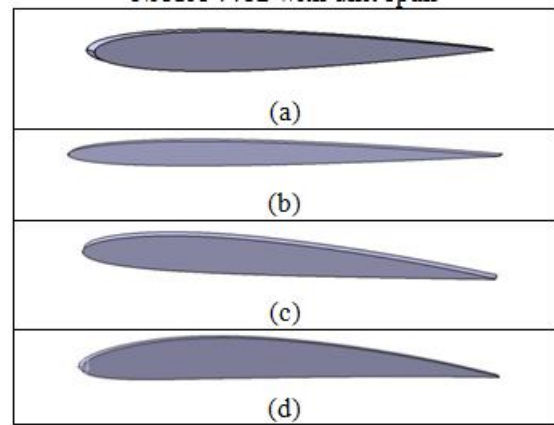


Fig 8 (a) NACA 0012 (b) NACA 1412 (c) NACA 2412 (d) NACA 4412 with unit span

VI. RESULT AND DISCUSSION

In this section, results obtained from numerical simulations performed to observe the effect of modified PBCF in increasing hydrodynamic efficiency of marine propeller is discussed. With a concept of guide vane in case of turbine, aerofoil shape propeller boss cap fin has been introduced. Aerofoil shape PBCF helps to generate more uniform flow in the hub vortex dominated zone and effectively increase hydrodynamic efficiency of the propeller. Simulations are performed on four separate aerofoil (NACA0012, NACA1412, NACA2412, and NACA4412) shape PBCF and the most efficient PBCF among them is identified. It has been observed that except NACA0012, in every aerofoil shape PBCF there is improvement in hydrodynamic efficiency. This is because in every case there are increases in thrust coefficients (K_T) as well as required torque coefficients (K_Q) and the percentage of increased K_T is quite high compared to require K_Q except as mentioned in NACA0012. The details of produced thrust, required torque and efficiency are shown in table 6. From table 5, it can be clarified that in case of NACA 0012, increased K_T is about 5% less compare to increase in K_Q , as a result there is an overall 2.64% decrease in efficiency as shown in fig.9

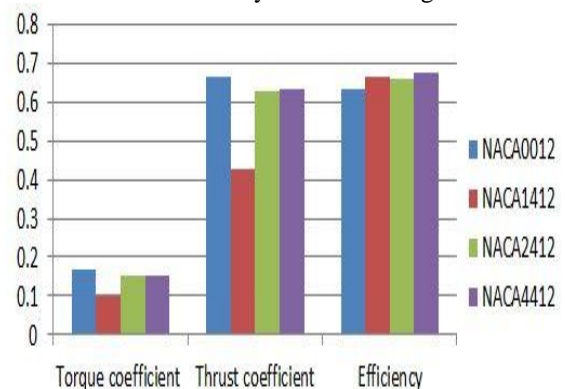


Fig. 9 Graphical representation of propeller characteristic with different PBCF

Further numerical investigations are carried out with NACA4412 profile to observe

Numerical Analysis Of Aerofoil Shape Propeller Boss Cap Fin (PBCF) To Improve Propeller Efficiency

its effect at various speed ratios. It has been noticed that NACA4412 profile PBCF starts to show significant improvement in propeller efficiency with advance ratio (J) nearby 1. However it produces a negative effect before J=1. This is because at lower velocity these PBCF generate high drag which results in requirement of high torque compared to significant improvement in thrust, which results reduction of efficiency as shown in fig.10.

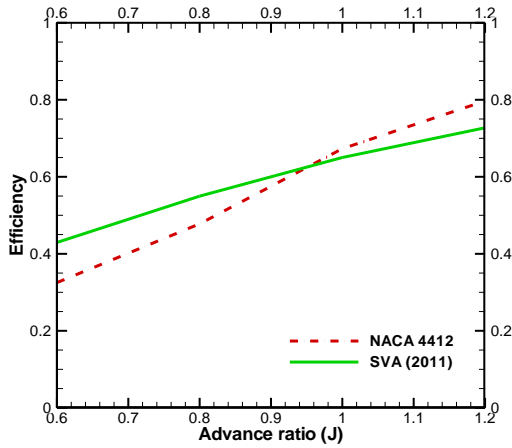


Fig. 10 Efficiency at various advance ratios with NACA4412

6.1 Pressure distribution

Pressure distribution on propeller surface from numerical simulations has been observed to perform a comparative study between the propeller without PBCF and with NACA4412 aerofoil shape PBCF. Propeller generates an axial thrust force due to the pressure difference between suction side and pressure side due to its aerofoil shape blade section profile.

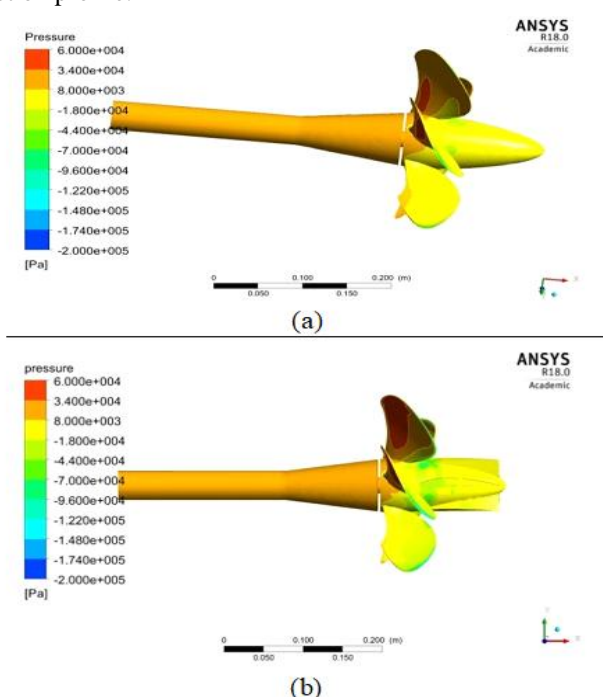


Fig. 11 Total pressure distribution on propeller blade surface (a) without fin (b) with fin

From fig. 11 it is clear that for both cases propeller without PBCF and with PBCF, a maximum pressure is generated on the pressure side and a minimum pressure on the suction side

at the blade tip. PBCF helps to create a higher maximum pressure (55050 Pa) on the pressure side as compared to propeller without PBCF (41030 Pa) and thus a higher pressure difference is created between suction and pressure side. From fig. 11, it is also noted that the zone of maximum pressure generation on the pressure side is comparatively wider with PBCF than conventional propeller. Pressure distribution, surrounding the propeller is also investigated at various positions. To study these, four separate planes are considered perpendicular to propeller axis i.e X axis, namely at central plane, 0.1m before central plane and 0.1m, 0.2 m after propeller central plane as shown in fig 12. From fig. 10 it can be seen that pressure gradually decreases without PBCF as well as with PBCF after the propeller central plane, which leads to generation of high thrust. Contour of Fig. 13 (c) and (d) show PBCF helps to generate a low pressure at the propeller centre plane surrounding the blade tip and it becomes more in case of propeller with PBCF. This low pressure zone is becoming wider after the propeller part with the effect of aerofoil shape PBCF as shown in fig. 13 (f) and (h)

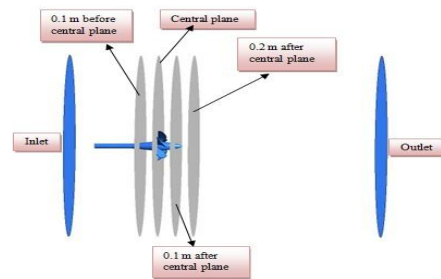


Fig. 12 various position of the considered plane

6.2 Velocity distribution

Fig. 14 shows introduction of PBCF significantly changes axial velocity distribution around the marine propeller across different planes as mentioned in pressure distribution. Velocity contour at the central plane clearly shows that the PBCF introduces a high velocity surrounding the propeller as shown in fig 14 (d). Besides, PBCF offers some resistive force at the root section which introduces a drag on that zone. The drag force offered by PBCF dominantly reduces velocity near hub section and due to its obstruction nature it significantly reduces the hub vortex at this zone. With the comparative study of fig 14 (e) and (f), it is seen that after the propeller central plane rate of velocity change with PBCF is more and fluid moves more rapidly at centre than conventional propeller. Along with the axial velocity component tangential velocity is also investigated to observe the effect of hub vortex. From fig. 15 it is clear that PBCF plays an important rule to reduce tangential velocity component surrounding the propeller hub and thus reduce hub vortex significantly.

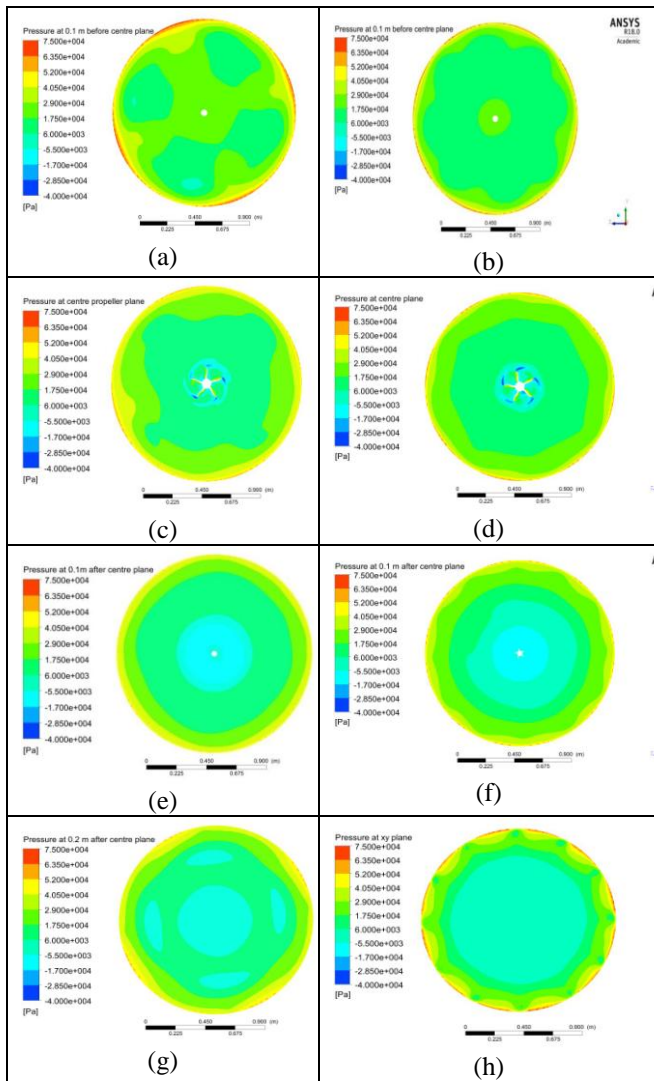


Fig. 13: Pressure contours at various positions (a) 0.1 m before the propeller central plane without PBCF (b) 0.1 m before the propeller central plane with PBCF (c) central plane of propeller without PBCF (d) central plane of propeller with PBCF (e) 0.1 m after the propeller central plane without PBCF (f) 0.1 m after the propeller central plane with PBCF (g) 0.2 m after the propeller central plane without PBCF (h) 0.1 m after the propeller central plane with PBCF

6.3 Hub vortex

A large amount of energy is lost due to the formation of strong swirl around the propeller hub and this leads to significant reduction of propeller thrust. According to Alter *et al.* [18], this hub vortex generates a higher magnitude of tangential velocity of water around the hub in reverse direction and a secondary vortex is created for flow passage on both side of the blade at root portion which creates a pressure difference. The main purpose of PBCF is to reduce the hub vortex by reducing pressure difference at the blade root and destroying swirl motion surrounding the propeller hub. In fig 16 (a) a strong hub swirl appears surrounding the propeller hub in case of propeller without PBCF, whereas this swirling flow quite vanishes in fig 16(b) with the application of NACA 4412 type PBCF. This results for significant improvement in propeller thrust as well as propeller efficiency. To capture more details about the flow behavior

surrounding the propeller and to study the effect of introduced PBCF, computational streamlines are observed in the fluid domain. From fig. 17 (a) and (b) it is clearly seen that with application of PBCF the number of swirling streamline reduces in comparison to those without PBCF and thus generate smoother flow surrounding the hub as well as after the propeller. These reductions in swirling flow significantly improve propeller efficiency by reducing energy loss and increasing propeller thrust.

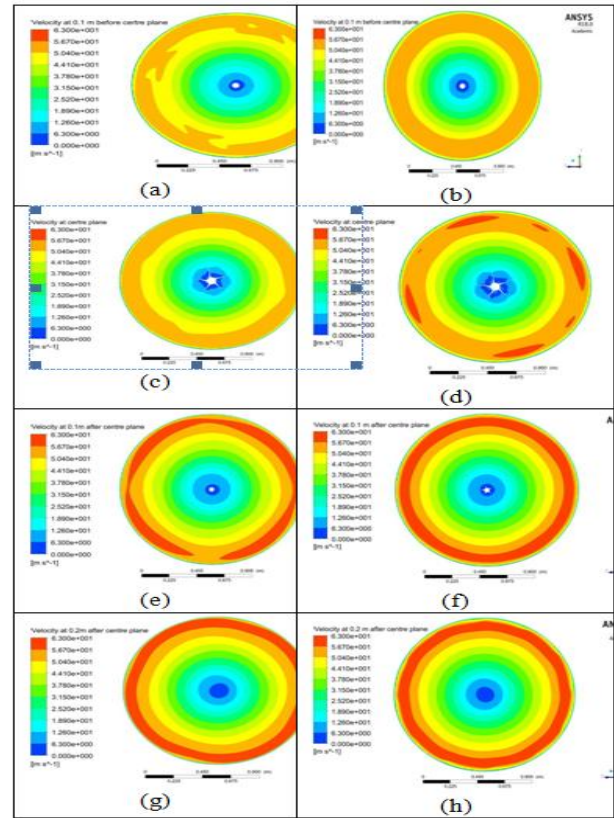


Fig. 14 Velocity distribution at various positions (a) 0.1 m before propeller central plane without PBCF (b) 0.1 m before propeller central plane with PBCF (c) central plane of propeller without PBCF (d) central plane of propeller with PBCF (e) 0.1 m after the propeller central plane without PBCF (f) 0.1 m after the propeller central plane with PBCF (g) 0.2 m after the propeller central plane without PBCF (h) 0.1 m after the propeller central plane with PBCF

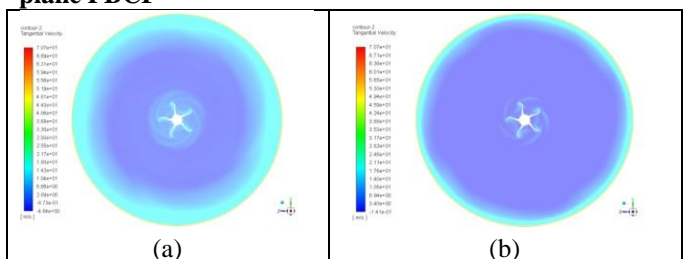


Fig. 15 Tangential velocity at centre plane (a) without PBCF (b) with PBCF

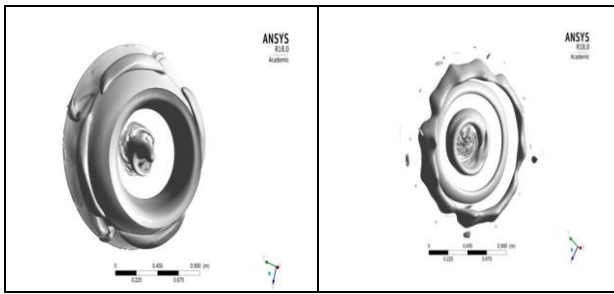


Fig. 16 Vortices (a) without PBCF (b) with PBCF

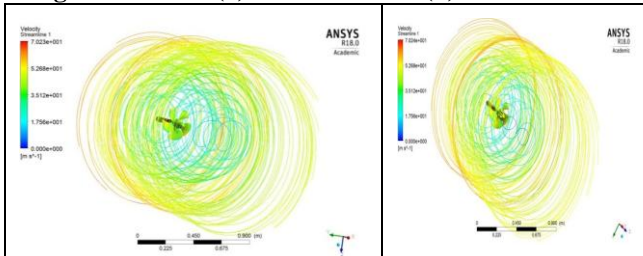


Fig. 17: Streamline flow around propeller (a) without PBCF (b) with PBCF

VII. CONCLUSION

This paper presents a numerical investigation using CFD to predict the effect of aerofoil shape PBCF to improve propeller efficiency. The CFD calculation has been performed with four separate type of aerofoil shape PBCF namely NACA0012, NACA 1412, NACA2412 and NACA4412.

For confirmation of numerical solver validation study has been carried out and reasonable agreement with experimental results of SVA (2011) is observed. Validation study is performed with sliding mesh as well moving reference frame (MRF) approaches showed quite similar results. However less consumption of computational time encouraged all the simulations to be performed in MRF approach. Numerical simulation carried out with all cases of aerofoil shape PBCF (except NACA0012), showed improvement in efficiency improvement with maximum of 3.52% in case of NACA4412 than without PBCF propeller. Pressure distribution showed that there are significant pressure differences created between suction side and pressure side which increases the thrust and due to the shape of the PBCF considered, significant drag to the flow field and thus required torque were also produced. However the combined effect of thrust and torque improvement showed an overall propeller efficiency improve. It is also seen that PBCF drastically reduces hub vortex which is the cause for energy losses while in practical situations. Analyzing streamline around the propeller it has been found that the number of swirling streamlines surrounding the propeller hub reduces with the introduction of aerofoil shape PBCF. This paper suggest a better improvement of propeller efficiency through the application of aerofoil shape PBCF compare to previous PBCF as discussed in literature (Mizzi *et al*^[14]).

REFERENCES

1. D. Owen, Demirel., Y. K. Oguz, T. Tezdogan and A Incecik. "Investigating the effect of biofouling on propeller characteristics using CFD". *Ocean Engineering*, 2018, 159: 505–516.
2. J. S. Go, H.S. Yoon and J. H. Jung. "Effects of a duct before a propeller on propulsion performance". *Ocean Engineering*, 2017, 136: 54-66.

3. G. Dubbioso, R. Muscari and A. D. Mascio. "Analysis of a marine propeller operating in oblique flow. Part 2: Very high incidence angles". *Computer & Fluids*, 2014, 92: 56-81.
4. L. X. Hou, C. H. Wang, A. K. Hu and F. L. Han. "Wake-adapted design of fixed guide vane type energy saving device for marine propeller". *Ocean engineering*, 2015, 110: 11-17.
5. T. Kawamura, K. Ouchi and S. Takeuchi. "Model and full scale CFD analysis of propeller boss cap fins (PBCF)". *Third international symposium on marine propulsors smp*, Launceston, Tasmania, Australia, May 2013, 486-493.
6. MOL to Launch Sales of Redesigned, Refined PBCF - Meeting Higher Needs for Environmental Protection by Further Improving Energy-saving Performance. 2017 (<http://www.mol.co.jp/en/pr/2017/17030.html>).
7. Walker and D. L. Norris. "The influence of blockage and cavitation on the hydrodynamic performance of ice class propellers in blocked flow (microform)". Thesis (Ph. D.)-Memorial University of Newfoundland, 1996.
8. T. Nojiri, N. Ishii. and H. Kai. "Energy Saving Technology of PBCF (Propeller Boss Cap Fins) and its Evolution". *Journal of the JIME*, 2011, 46: 63-71.
9. T. Kawamura, K. Ouchi and T. Nojiri. "Model and full scale CFD analysis of propeller boss cap fins (PBCF)". *J Mar Sci Technol*, 2012, 17: 469–480.
10. Y. Xiong, Z. Wang and W. Qi. "Numerical Study on the Influence of Boss Cap Fins on Efficiency of Controllable-pitch Propeller", *Journal of Marine Science and Application*, 2013, 12: 13-20.
11. S. Lim, T. Kim, D. Lee, C. Kang. and S. Kim. "Parametric study of propeller boss cap fins for container ships". *Int. J. Nav. Archit. Ocean Eng.* 2014, 6: 187-205.
12. S. Park, B. Han and B. Chang. "A study on the propulsive performance on HI-Fin". The 12th international conference on hydrodynamics, 18-23 September 2016, Egmond aan Zee, Netherland.
13. Y. Sun, Y. Su, X. Wang and H. Hu. "Experimental and numerical analyses of the hydrodynamic performance of propeller boss cap fins in a propeller-rudder system. *Engineering applications of computational fluid mechanics*, 2016, 10 (1): 145–159
14. K. Mizzi, Y. K. Demirel, C. Banks, O. Turan, P. Kaklis and M. Atlar. "Design optimisation of Propeller Boss Cap Fins for enhanced propeller performance". *Applied Ocean Research*, 2017, 62: 210–222
15. Schiffbau-Versuchsanstalt Potsdam GmbH (SVA) Potsdam Model Basin. Potsdam propeller test case (PPTC). Open Water Tests with the Model Propeller VP1304, April 2011, report no. 3752.
16. R. Koirala, H.P. Neopane, S. Oblique, B. Zhu and B. Thapa. "Selection of guide vane profile for erosion handling in Francis turbines", *Renewable Energy*, 2017, 112: 328-336
17. K. Ouchi, M. Ogura, Y. Kono, H. Orito, T. Shiotsu, M. Tamashima. and H Koizuka. "A research and development of PBCF (propeller boss cap fins)-improvement of flow from propeller boss". *Journal of the Society of Naval Architecture of Japan*, 1988, 163: 66-78.
18. M. Atlar and G. Patience. "An investigation into effective boss cap designs to eliminate propeller hub vortex cavitation". *Proceedings of the 7th International Symposium on Practical Designs of Ship and Mobile Units* 1998; 757–769.

AUTHORS PROFILE



Pritam Majumder, Research scholar in Mechanical Engineering from NIT Meghalaya, India. Main interest of research in fluid mechanics. Completed masters from NIT Silchar Assam India.



Dr. Subhendu Maity, assistant professor in department of mechanical engineering NIT Meghalaya. Ph. D, IIT Kharagpur, Research interest in Turbulence Modeling, Fluid Mechanics, Computational Fluid Dynamic.